Overturning of multiple-block stacks - dynamic sensitivity parameters and scaling effect

Nina Čeh*, Nenad Bićanić*, Jean-Francois Camenen*, Antonio Pellegrino[+], Nik Petrinić[+]

*Faculty of Civil Engineering, University of Rijeka, Radmile Matejčić 3, Rijeka, Croatia
E-mails: {nina.ceh,nenad.bicanic,jfcamenen}@uniri.hr

[+]Department of Engineering Science, University of Oxford, Parks Road, Oxford
E-mails: {antonio.pellegrino,nik.petrinic}@eng.ox.ac.uk

Abstract

Both experimental and computational dynamic sensitivity study of multiple-block stacks subjected to a double pulse base excitation are examined. Series of test experiments were conducted at the Oxford Impact Engineering Laboratory on a bespoke platform for a controlled double (initial and inverse) pulse base excitation history. For the computational simulations and validation the base of the block stack was subjected to a constant acceleration of a finite duration until the desired peak base velocity, corresponding to the measured experimental values, was achieved. Different overturning modes (forward, backward, global and partial) in both simulations and experiments were characterised as a function of the peak initial base velocity and the timing of the reverse impulse, controlled by the stop gap distance between the base and the stopper. The influence of the block sample scales has also been examined. The conducted set of validation benchmarks is believed to be valuable for researchers, code developers, safety case engineers and industry regulators.

Introduction

In order to better understand as well as to predict the highly nonlinear mechanical response of natural and/or engineered discontinuous, blocky structures, comprising evolving contact conditions and including friction between their components or constituent parts, it is important to develop robust analytical capabilities for simulations of such systems. In spite of extraordinary advances in nonlinear computational mechanics and simulations paradigms, the validation and verification of their predictive powers remains one of the main challenges in order to promote their incorporation into the industry relevant procedures. It can be

safely argued that a major research attention in nonlinear structural dynamics today has noticeably moved from considering a detailed response of a very specific structural system to a defined excitation, towards a more generic predictive capability for a class of structural configurations.

There are a number of structures that are inherently discontinuous, either as a matter of convenience (e.g. ease of construction in structural masonry or dry stone walling) or as a deliberate strategy to avoid extensive thermal stresses (e.g. graphite cores in Advanced Gas-cooled Reactors, AGR, in nuclear power plants). Often these structures are organised as stacked and/or interlocked assemblies with a regular pattern and technologically intended gaps and clearances, allowing for limited sliding and rocking in between contacts during their dynamic response. Frequently, these structural assemblies represent by themselves a vital safety critical component (or form a crucial part) of an entire structural system and there is a growing need to be capable to predict their behaviour under both static and dynamic (impact, seismic) conditions. This is particularly true with ageing and degradation of such systems (e.g. AGR cores), where the safety considerations with respect to their life extension may be paramount for the integrity assessment process of the entire plant operation. Moreover, some of the safety critical 'non-structural' components (e.g. large control cabinets) need to be treated as unanchored or partially anchored blocky structures in their seismic assessment.

Direct extension of the structural reliability and integrity assessment procedures developed for continuous structures to include also discontinuous structural assemblies is clearly not appropriate. Considerations of blocky systems therefore often rely on some form of a homogenisation technique (simplified or complex), leading to a whole series of equivalent nonlinear continuum models. Such idealisations then follow well established routes, developed for continuum structures and supported by a series of well recognised benchmarks, both computational and experimental. In particular, the homogenisation process allows for a reasonably straightforward dynamic characterisation (e.g. spectral signature, eigen frequencies and mode shapes for response spectrum techniques in earthquake considerations are easily evaluated) of systems which are in reality discontinuous, 'blocky' structures, for which no eigen-problem can be formulated.

Title

Blocky Structures

Dynamic behaviour of blocky structures has been addressed extensively in the past and it keeps on attracting a lot of research efforts. Since the pioneering seminal work by Housner (Housner, 1963) on the overturning of a single rigid block, there have been numerous contributions (Dimitrakopoulos and DeJong, 2012; Hogan, 1994; Lopez Garcia and Soong, 2003; Makris, 1998; Pena et al, 1992; Psycharis and Jennings, 1983; Yim et al., 1980; Zhang and Makris, 2001), with the base excitation ranging from constant acceleration, harmonic excitation to complex earthquake type signals. Different approaches were recorded (analytical, computational, experimental) with the whole range of complexities or simplifications on the blocks contacts (rocking, sliding, uplifting, energy dissipation during block collisions). Strictly analytical consideration is predominantly confined to the study of the rocking motion and overturning conditions of a single block or a stack of blocks comprising a relatively small number of blocks, as the complexity of possible configurational changes rises dramatically (Kounadis et al., 2012; Pena and Campos-Costa, 1992; Psycharis, 1990; Spanos et al., 2001) The more complex blocks assembly is considered, there is generally far less information available about experimental findings and comparison with either analytical or computational predictions.

This contribution comprises preliminary results of both the experimental and computational dynamic sensitivity study about the nature of a single block and multiblock stack overtopping modes (global or partial), when subjected to a very distinct base excitation – a controlled double pulse base excitation. The key research questions are

- to examine the double pulse conditions (initial impulse, followed by a reverse shock after some time delay) needed to induce the reverse direction overtopping mode of a single block, following the initial rocking,
- to explore the double pulse base excitation conditions (impulse intensities and time delay) leading to the partial overturning of a multi block stack (top block overtopping, equivalent to a ‘higher mode’ failure in continuum structures),
- to establish if the conditions for partial overturning can be scaled from one size to another for geometrically similar block sizes and

- to furnish a set of well controlled and well documented benchmarks to be used for the validation of computational simulations.

Experimental set-up and simulation platform

Experimental set-up and preliminary notes

In the context of a joint research project between the universities of Rijeka, Durham and Oxford, a comprehensive series of experiments was conducted at the Oxford Impact Engineering Laboratory on a bespoke platform for a controlled double pulse base excitation, inspired by the classic ingenious simple experimental test device at Roorkee University (Qamaruddin et al., 1984), where the railway wagons on inclined planes and hellical springs were used to generate varying controlled double half sine pulse base excitations and the associated input kinetic energy was correlated to a scalar measure of damage experienced by the test structures (Figure 1).

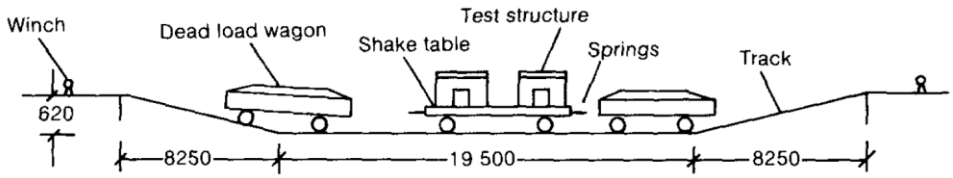

Figure 1. Schematic view of the Roorkee University test facility (7)

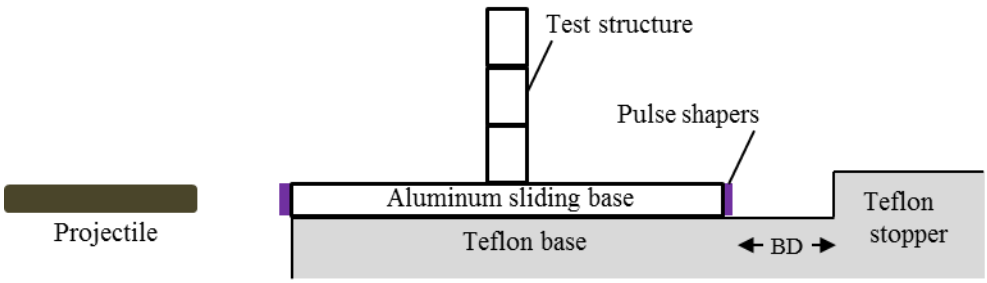

Figure 2. Schematic view of the ROORI-1 test facility in Impact Engineering Laboratory, University of Oxford

The experimental setup at the University of Oxford (named ROORI-1 as an homage to both Roorkee and Rijeka Universities) comprised an impact device based on a pin-ball mechanism with a spring used to launch a wooden projectile,

with a Teflon PTFE base and a stopper aligned to the impact device and attached to the optical bench (Figures 2 and 3).

An aluminium sliding base, sitting on the low friction teflon PTFE surface was positioned at a predefined distance from the stopper (BD). The dimensions of the sliding base were the following: length 0.2 m, width 0.02 m and thickness 0.01 m. The base excitation was triggered with an initial impulse (different intensities were controlled by the different initial pin-ball spring positions) followed by a reverse impulse (provided by the base hitting the stopper), after a given time delay (controlled by the distance between the base and the stopper). The wooden projectile used to induce the impulse was of a cylindrical shape with a length of 0.079 m, a diameter 0.0179 m and a mass of 0.0081 kg. A rubber cushion was glued to the front and the back face of the aluminium base to act as a pulse shaper.

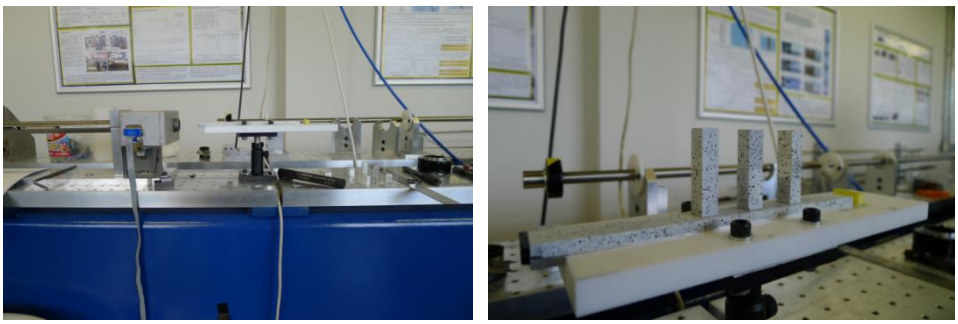

Figure 3. Optical bench and ROORI-1 test facility (left); samples of multi-block structures on the sliding base (right)

On top of the sliding base the test structure (either a single block or a stack of three blocks) was positioned and aligned to the projectile and the teflon PTFE base (Figure 3, left). Surface roughness of the sliding base-block interface and of each of the inter-block surfaces was achieved by using sandpaper with P60 grit (scraping aluminium surface along the sandpaper surface), to exclude sliding. Simple experiments showed the inter-blocks and the block-base surfaces with the friction coefficient of 0.54, while the friction coefficient between the sliding base and the Teflon PTFE surface was 0.23.

All the experiments were triggered manually and a good repeatability was achieved, however the results for some experimental scenarios appeared to be quite sensitive to small changes in initial conditions.

Author

Advanced non-contact optical measuring technique based on the GOM Aramis and Pontos system (MbH G. Aramis; Pickerd, 2013) and the corresponding processing software have been applied to replace conventional displacement measuring systems. Every experiment was recorded with either the Phantom or the Photron video camera with a resolution of 800x600 pixels and a frame rate of 2000 fps. The camera was triggered by a laser-beam curtain. Every video was converted into a series of images (in .jpg format). Each series of images was post processed using GOM Aramis v6.3.1 software for optical deformation and displacement analysis. GOM Aramis software is based on dividing the image of the experiment into facets (rectangular units with a unique arrangement of dark and light pixels) which are traced through the set of images extracted from the video in order to conduct the information of displacements and deformations on the surface of the tested sample (Pickerd, 2013). Given the resolution of the images of 800x600 pixels, each pixel represented approximately a 0.18 mm side square. Choice for the facet size needed to be optimised, as it depends on the sample surface speckle pattern, pixel size and the scale of observation.

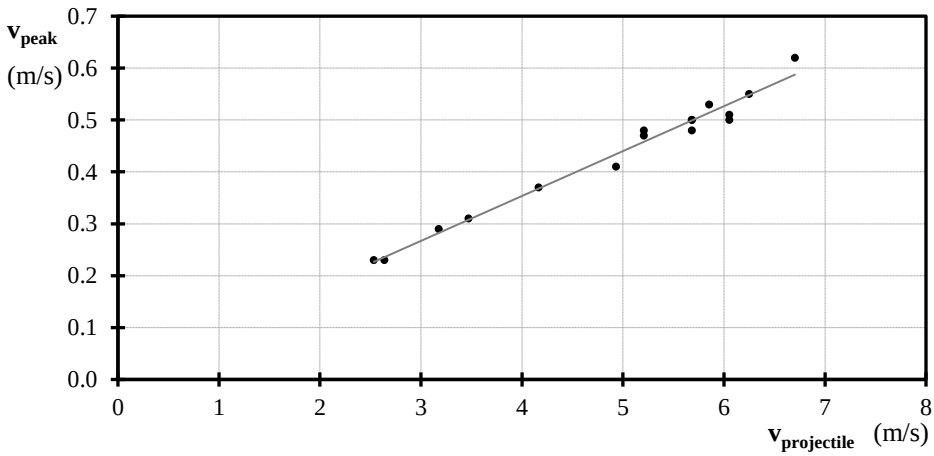

Figure 4. Peak base velocity vs. projectile velocity just before the impact

The input impact energy and projectile velocity is imparted to the sliding base. The resulting post first impact peak base velocity, achieved after a very short rise time, reflects not only the initial projectile position but also the consequences of the energy dissipation during impact, on the projectile/base mass ratio and the influence of the rubber cushion. Both the incoming projectile velocity and the post

impact base velocity were measured (by means of two laser courtains with given distance and optical system), and a seprate restitution study concluded that the peak base velocity post first impact was directly proportional to the projectile velocity (Figure 4) irrespective of the projectile velocity level, corresponding to a constant restitution.

Computational Simulations

There are a number of computational simulation paradigms relevant for multiple-block structural configurations with clearances, both within the explicit and the implicit contact dynamics time integration settings. The DEM (Discrete Element Method) (Cundall and Strack, 1979), in particular the UDEC and 3DEC frameworks (UDEC&3DEC) and LS-DYNA (LS-DYNA) have largely been accepted as industry standard, despite their lengthy computational times, associated with extremely small time integration steps, controlled by the conditional stability of explicit schemes. Up until relatively recently, the implicit contact dynamics computational realisations, where the non-interpenetration contact conditions need to be simultaneously satisfied for every contact at every time step, were neither practical nor competitive for engineering practice, as the iterative processes rendered far too excessive total simulation times. The explicit and implicit simulation paradigms also differ in terms of the computational treatment of contact energy dissipation. However, significant advances in efficient iterative solvers and nonlinear optimisation algorithms, have improved implementations of the implicit non-smooth contact dynamics paradigms and significantly reduced the solution times, bringing them very close to the durations acceptable for realistic engineering applications, previously reserved for the explicit frameworks.

Within this contribution, comparative Non Smooth Contact Dynamics (NSCD) studies were conducted with SOLFEC http://code.google.com/p/solfec/ (Koziara and Bićanić, 2011; SOLFEC), as a representative of an implicit simulation framework for contact dynamics. SOLFEC employs the Contact Dynamics paradigm (Jean, 1999) in the context of multiple bodies. There are discontinuities in the velocities field, and the NSCD framework recasts the entire problem in terms of *differential measures* or *distributions*, i.e. without the need to define the acceleration as a usual derivative of velocity. Instead of using the regularised form of dynamic equations of equilibrium, the ‘non-smooth’ time discretized form of

dynamic equations is obtained by integrating the dynamic equation, so that the velocities become the primary unknowns

$$M\left(\dot{x}_{i+1}-\dot{x}_i\right)=\int_{t_i}^{t_{i+1}}F(t,x,\dot{x})dt+\int_{t_i}^{t_{i+1}}rdt \qquad x_{i+1}=x_i+\int_{t_i}^{t_{i+1}}\dot{x}dt \tag{1}$$

Furthermore, the force impulse on the RHS is typically conveniently split into two parts, where the first integral (due to external forces only, hence excluding the effect of contact forces) is considered continuous, whereas the second part (the contribution of contact forces to the total force impulse) is replaced by the mean value impulse, acting over the finite time step interval. The NSCD simulation effectively ignores the high frequency content of the contact interactions (Koziara and Bićanić, 2011; Radjai and Richefau, 2009). Instead of a specified interpenetration-force relation, this paradigm employs the complementarity relation between the relative velocity and the contact impulse at an existing contact point. The velocity-impulse relation is added as an algebraic constraint to the implicitly integrated momentum balance and the ensuing nonlinear contact problem is therefore solved implicitly at every time step. More details can be found in various seminal references on the CD (Computational Dynamics) paradigm as a noon smooth discrete element method, listed in (Radjai and Richefau, 2009).

For the purpose of comparative simulations, the base was subjected to a constant acceleration (linear rise of velocity) over a fixed finite time interval (0.005 sec), giving rise to a series of different peak base velocities (Figure 5). All blocks were assumed to be rigid. Coefficient of restitution for both inter block and block base normal and tangential direction were set to zero. Coefficient of friction (aluminium base-teflon PTFE base) is adopted as 0.26. In the experiment, the surface of the blocks is considered either smooth or non-smooth after sandblasting. High coefficient of friction was adopted to prevent inter block sliding. Consequences of a series of different block and base grid subdivisions/discretisations were explored for the purpose of contact detection, as all the blocks are assumed rigid (Figures 5, 6 and 7).

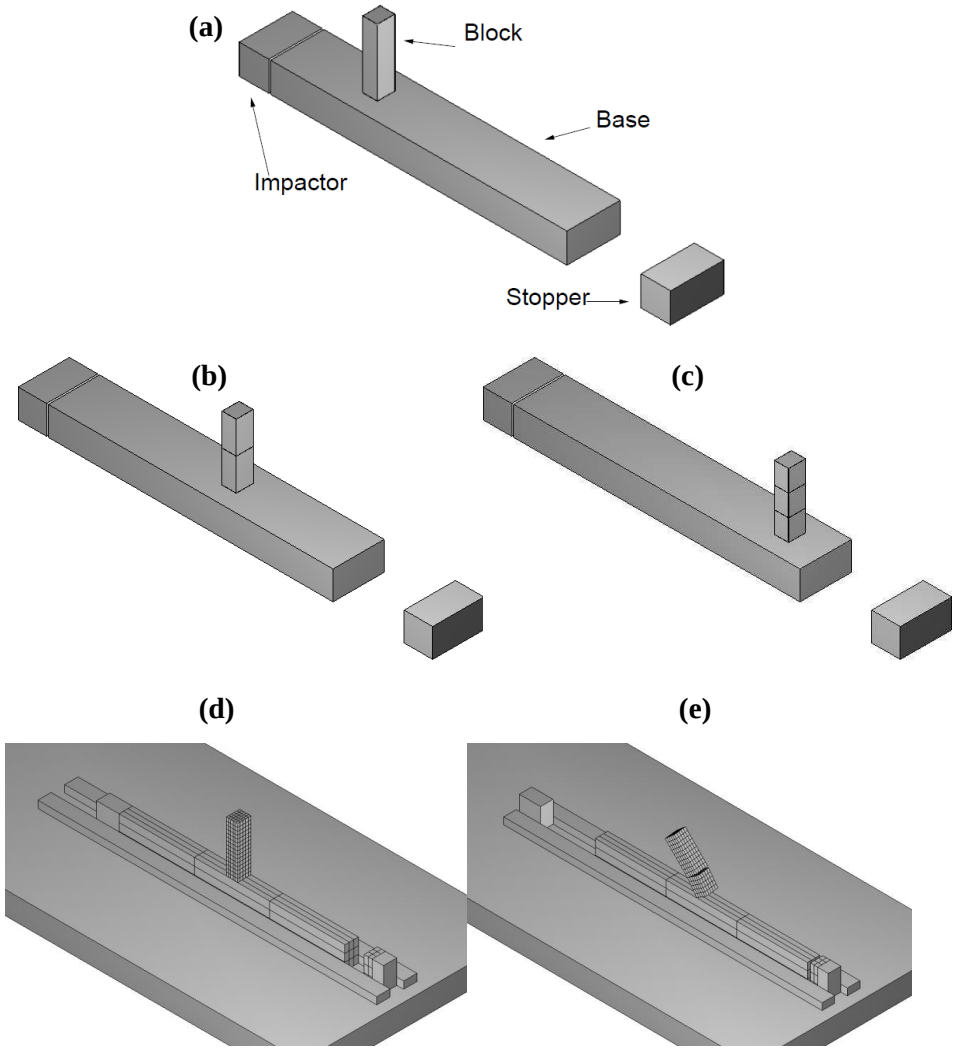

Figure 5. SOLFEC NSCD simulations of the ROORI-1 experimental setup: (a) simulation setup scheme, (b) bi-block and (c) three block structure with coarse discretization, (d) single block and (e) three block structure with dense discretization

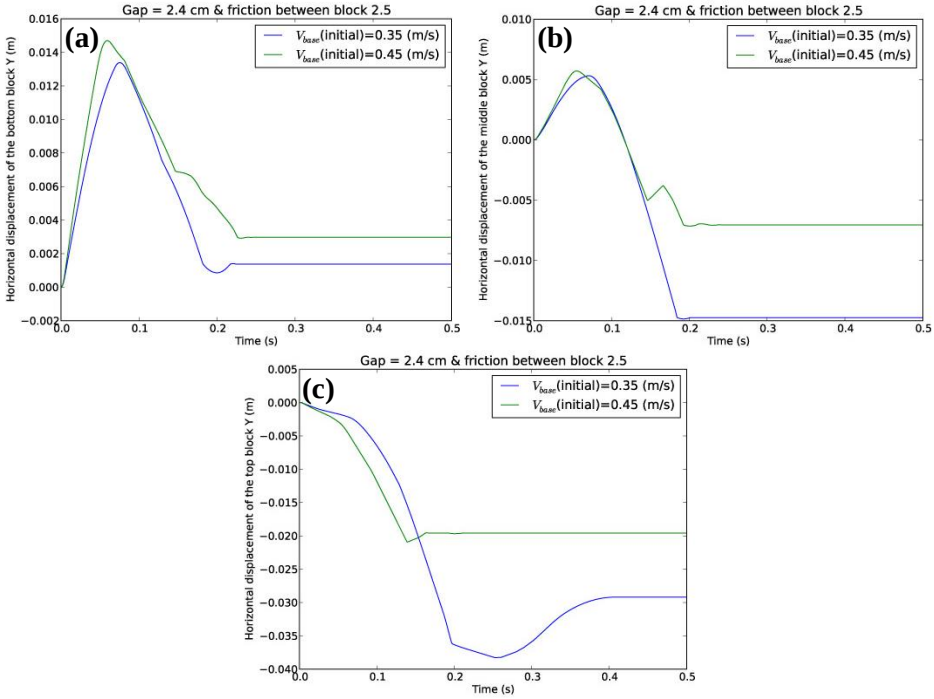

Figure 6. Horizontal displacement time histories for the (a) top, (b) middle and (c) bottom block centroid for the two pulse excitation scenarios with peak base velocities (0.35 m/sec and 0.45 m/sec)

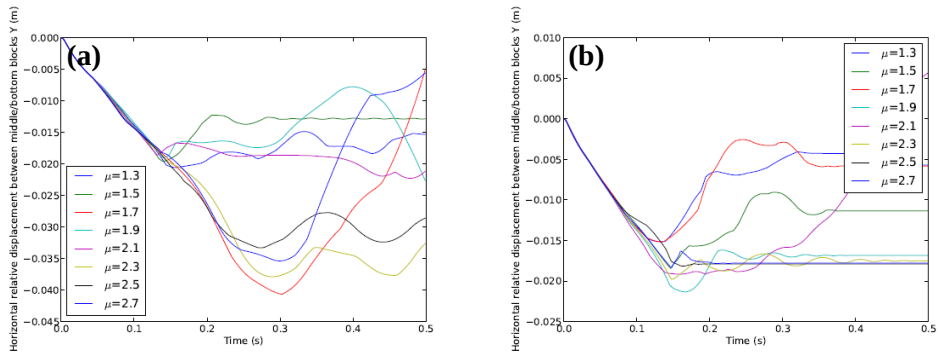

Figure 7. Time evolution of the horizontal relative horizontal displacement between the middle and bottom blocks, with (a) the grid (1, 1, 1) and (b) a finer grid (3, 3, 3)

Title

Controlled pulse excitation experiments and NSCD simulations

Single block study

A series of single aluminium block experiments subject to different double pulse type base excitations on two different scales were carried out. The dimensions of test samples at the smaller scale (Scale 1) were h_1=45 mm, b_1=10 mm and l_1=10 mm, whereas for the larger scale (Scale 2) the dimensions were h_2=90 mm, b_2=20 mm and l_2=20 mm. The final state of the samples as an outcome of the controlled double pulse was characterised by either its stable state or by a specific mode of overturning, for each experiment and for each simulation (see Figure 8):

- Mode of overturning **A** if the block remained stable at the end of the experiment and
- Mode of overturning $\mathbf{B_L}$ or $\mathbf{B_R}$ if the block overturned to the left or to the right side, respectively.

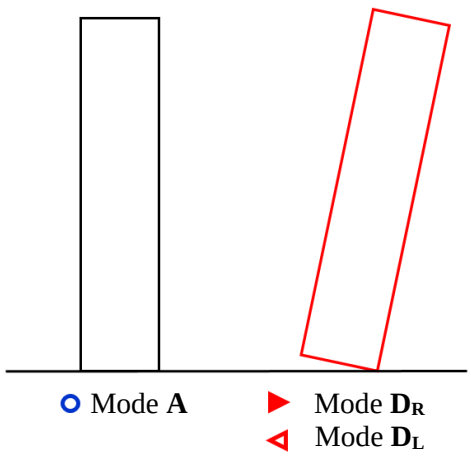

Figure 8. Modes of overturning of a single block structure

Single Block Study - Scale 1

Experimental results of the overturning behaviour for a single block (Scale 1) due to the double pulse-type base excitation are shown in Figure 9 as a relationship between the distance between the base and the stopper BD and the initial (peak)

sliding base velocity v_{peak}. For the low peak base velocities, the sliding base does not reach high enough velocity to overturn the block (experiments with projectile velocity of 0.1 m/s in Figure 4). For higher velocities the block starts rocking but in experiments where the distance between the sliding base and the stopper is small, the base experiences a reverse pulse, which results in an acceleration in opposite direction, causing the block to start rocking about the opposite corner. Such behaviour may eventually result in block stability even for very high velocity (left part of the graph in Figure 9).

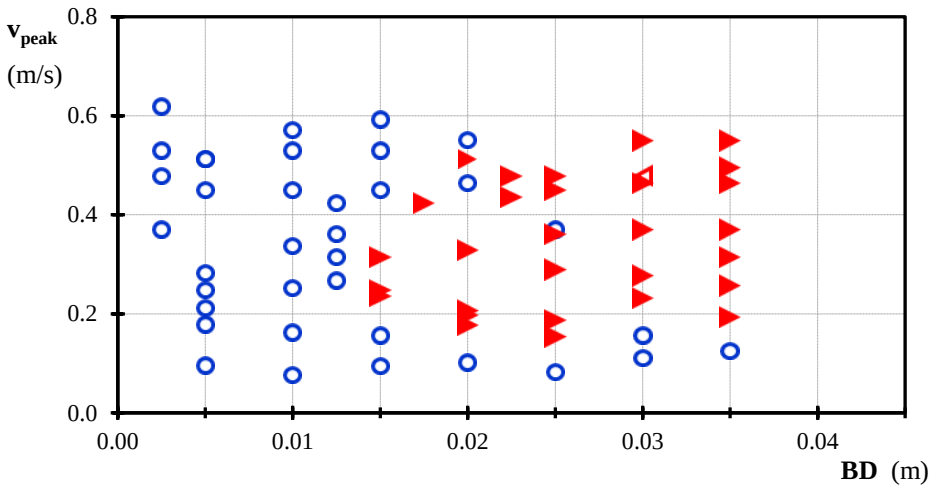

Figure 9. Modes of overturning of a single block structure (Scale 1) from experimental study

Results from the computational simulations of the single block overturning behaviour at scale 1 are shown in Figure 10, again illustrated as a relation between the sliding base to stopper distance BD and the peak base velocity.

Title

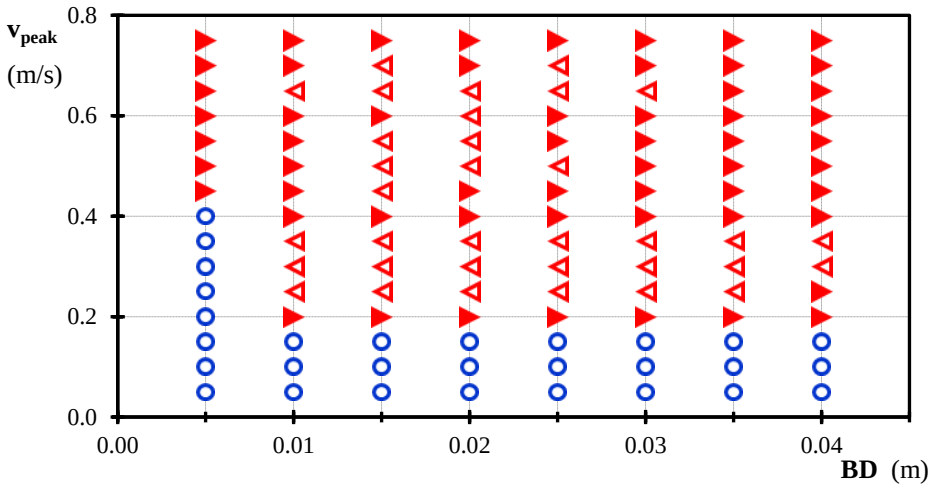

Figure 10. Modes of overturning of a single block structure (Scale 1) from computational simulation study

Simulations results indicated overturning of the block with initial conditions which during experiments resulted in block remaining stable, hence the simulations underestimate the region of stability of a single block, especially with respect to the stopper gap distance.

Single Block Study - Scale 2

Experimental results of the overturning behaviour of a single block at Scale 2 due to double pulse-type base excitation are shown in Figure 11 and the end states are characterised in the same way as the experiments at Scale 1. In comparison to the experimental results for the smaller single block larger velocities are required to overturn the larger block, as expected. Longer travel times (larger distances between the base and the stopper) lead to more stable behaviour for larger blocks.

Author

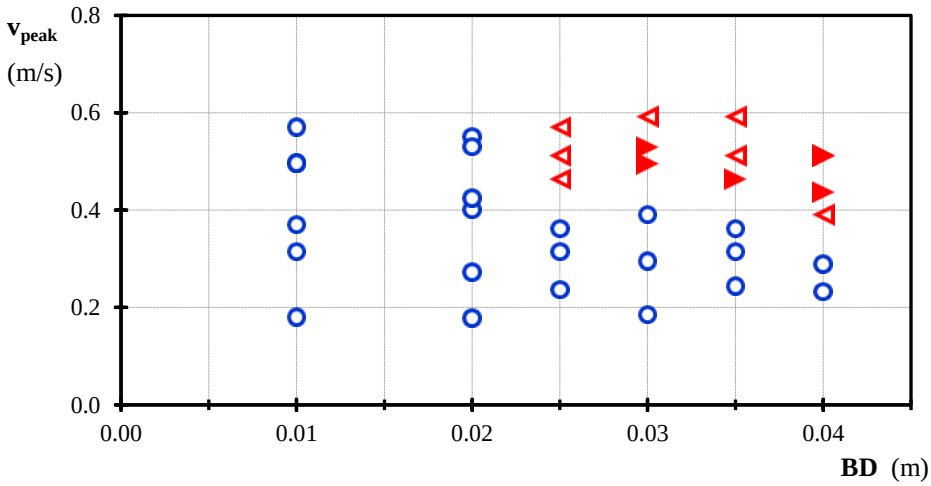

Figure 11. Modes of overturning of a single block structure (Scale 2) from experimental study

Computational simulations of the experiments at Scale 2 are shown in Figure 12.

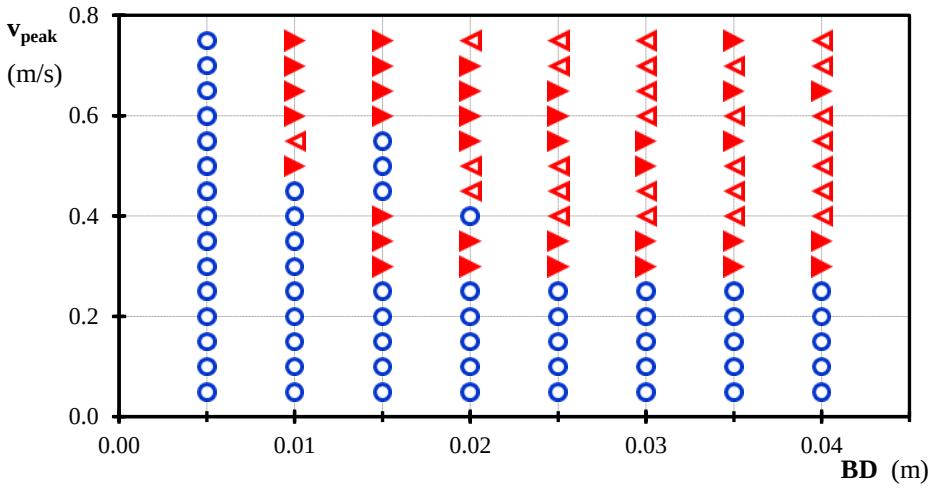

Figure 12. Modes of overturning of a single block structure (Scale 2) from computational simulation al study

Results from computational simulations are qualitatively comparable to experimentally obtained results with respect to the BD distance and the peak base

velocity, but simulations results suggest easier overturning of the block both with respect to BD and the v_{peak} than obtained from experiments.

Single Block Study – comments on the scaling effect

Scaling effect in rocking behaviour of blocky structures has been addressed in (Dimitrakopoulos and DeJong, 2012), where the angle of slenderness α was suggested to scale the amplitude of excitation. In this study with blocks on two scales it is clear that larger amplitude of excitation (impact type) is needed to overturn the larger block, whereas the angle of slenderness is the same for both scales. Results are plotted so that the amplitude of excitation is expressed as the input kinetic energy and scaled using the mass of the block (ratio of the larger block mass to the smaller block mass is m_2/m_1=6.83). Housner's frequency parameter p (Housner, 1963) was adopted to scale the frequency of the excitation The frequency parameter ratio of the larger block to the smaller block is p_2/p_1=0.707 and the period of excitation T_d can be estimated as the sum of the impulse duration and the analytically approximated free sliding time before the base reaches the stopper with the assumption of zero friction. The combined experimental results of blocks on both scales are shown in Figure 13.

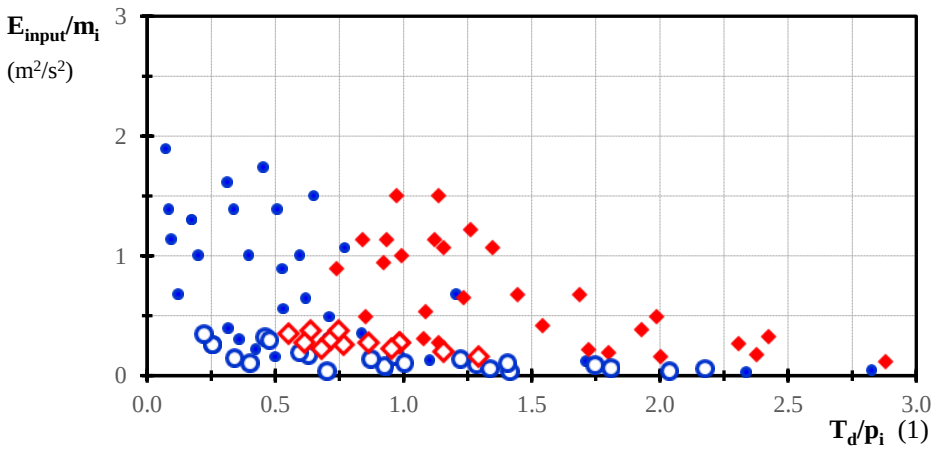

Figure 13. Areas of overturning (red marks) and no overturning (blue marks) for single block (Scale 1 is represented with filled marks, Scale 2 is represented with empty marks) obtained from experimental study

Equivalent combined results of the simulations with blocks on both scales are shown in Figure 14. It is clear from both figures that the input energy scaling does

not result in mapping of both sets of results onto the same region and, while it is clearly a more suitable scaling parameter that the angle of slenderness, it cannot be directly used to scale the critical excitation amplitude.

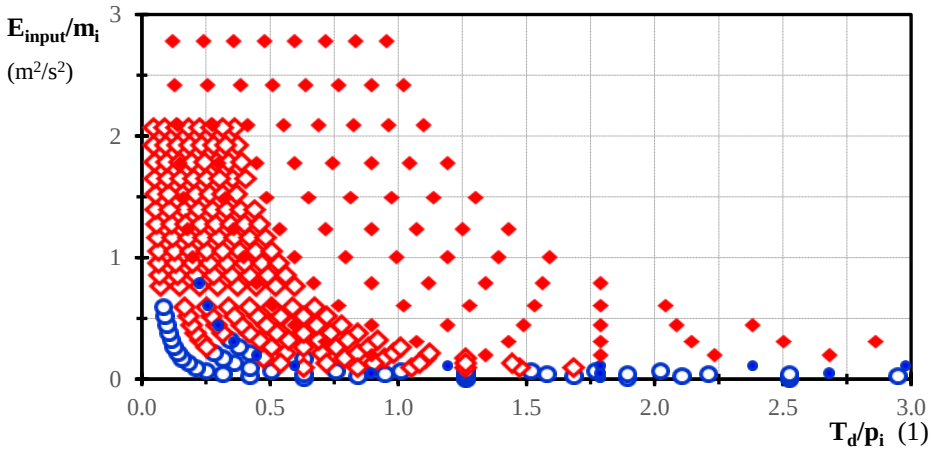

Figure 14. Areas of overturning (red marks) and no overturning (blue marks) for single block (Scale 1 is represented with filled marks, Scale 2 is represented with empty marks) obtained from computational simulation study

Multi Block Stack Study

A series of multi block stacks experiments on two different scales comprising three blocks, positioned one on top of the other, subject to a double pulse base excitation was carried out. Sample dimensions on the smaller scale (*Scale 1*) are h_1=15 mm, b_1=10 mm and l_1=10 mm, while the larger scale (*Scale 2*) samples dimensions are h_2=30 mm, b_2=20 mm and l_2=20 mm.

The end state for each experiment and for each simulation is again cathegorised using different modes of overturning (see Figure 15):

- Mode of overturning **A** if all the blocks from the stack remained stable at the end of experiment or simulation,
- Mode of overturning $\mathbf{B_L}$ or $\mathbf{B_R}$ if the top block from the stack overturned to the left or to the right side, respectively,
- Mode of overturning $\mathbf{C_L}$ or $\mathbf{C_R}$ if the two upper blocks from the stack overturned to the left or to the right side, respectively, and

- Mode of overturning $\mathbf{D_L}$ or $\mathbf{D_R}$ if the whole stack overturned to the left or to the right side, respectively.

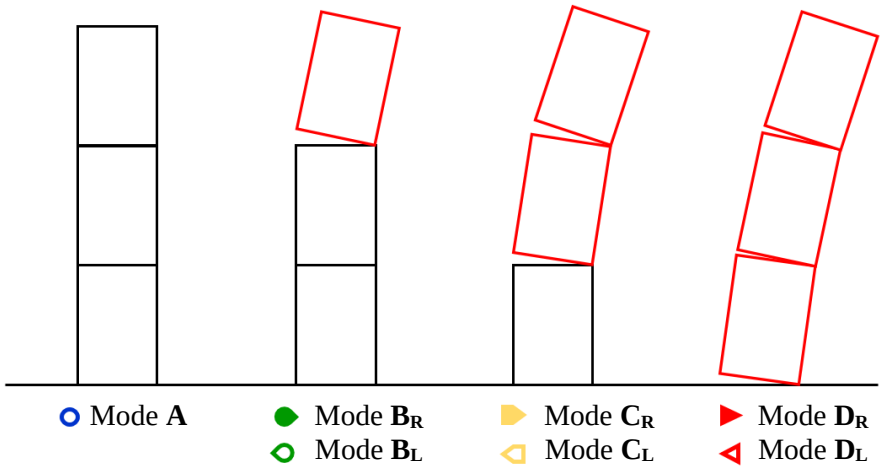

Figure 15. Modes of overturning of a three-block structure

Multi Block Study - Scale 1

Experimental results of the overturning behaviour of the stack of three blocks (Scale 1) due to pulse-type excitation are shown in Figure 16. Impacts with the projectile with velocity lower than 3.5 m/s are not resulting in overturning of any of the blocks. Impacts with higher velocities result in different modes of overturning (Figure 16).

Author

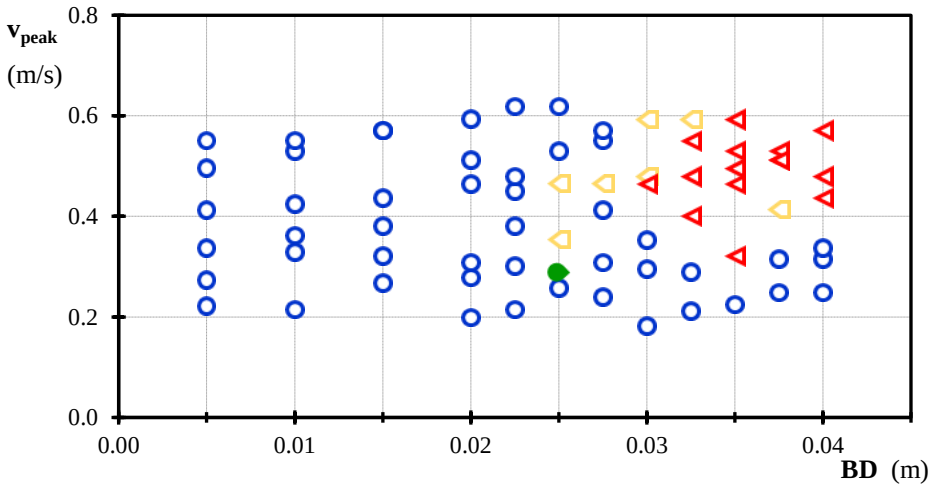

Figure 16. Modes of overturning of a three-block structure (Scale 1) from experimental study

Results from the corresponding computational simulations of rocking behaviour at Scale 1 are shown in Figure 17. Simulations appear to underestimate the stability range of the stack of three blocks, both in term of the distance between the base and the stopper and the peak velocity of the base (i.e. in experiments blocks remain stable for larger impact velocities). Experiments indicate that larger impact velocities than the ones resulting from simulations are required to overturn the block and the distance between the base and the stopper (controlling the travel time before the counter-shock) can eventually result in the stack stability even for stronger impacts (the left part of the graph in Figure 16 shows a stable stack, while the left part of the graph in Figure 17 shows different modes of overturning).

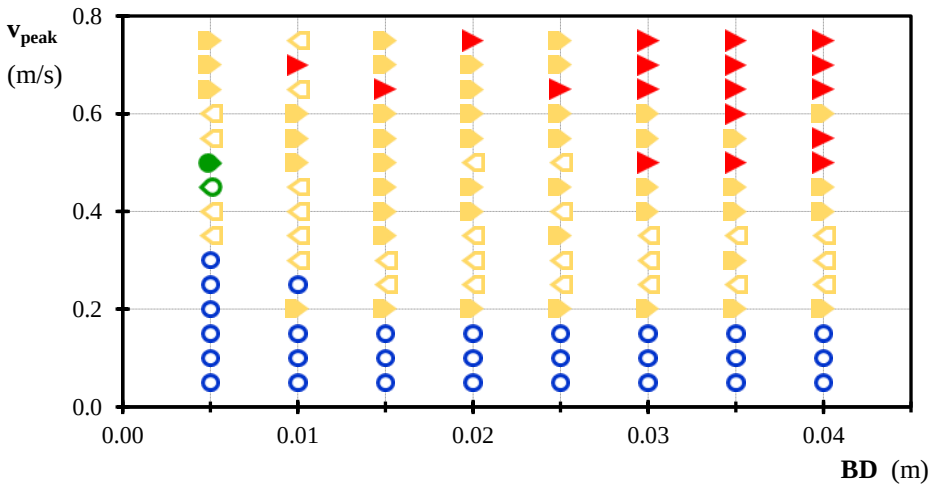

Figure 17. Modes of overturning of a three-block structure (Scale 1) from computational simulation study

Multi Block Study - Scale 2

Experimental results of the overturning behaviour of a stack of three blocks (Scale 2) due to the pulse-type excitation are shown in Figure 18. In comparison to the experimental results for the stack of smaller blocks, the stack with larger blocks requires higher projectile velocitties and consequently higher base velocities to overturn. The stack with larger blocks indicates a larger stability region with respect to the distance between the base and the stopper.

Author

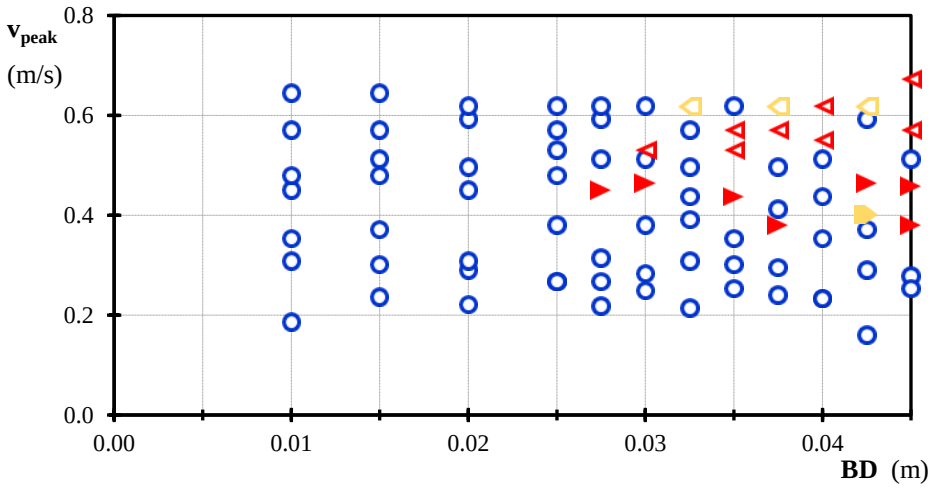

Figure 18. Modes of overturning of a three-block structure (Scale 2) from experimental study

Results from corresponding computational simulations of the overturning behaviour for Scale 2 are shown in Figure 19. The regions of multi stack instability obtained from the simulation and the experiments are more comparable for the larger stack of blocks (Scale 2) than for the smaller scale, even though the modes of overturning are different. Peak base velocity required to overturn the stack of blocks (Scale 2) obtained from experiments and computations is comparable.

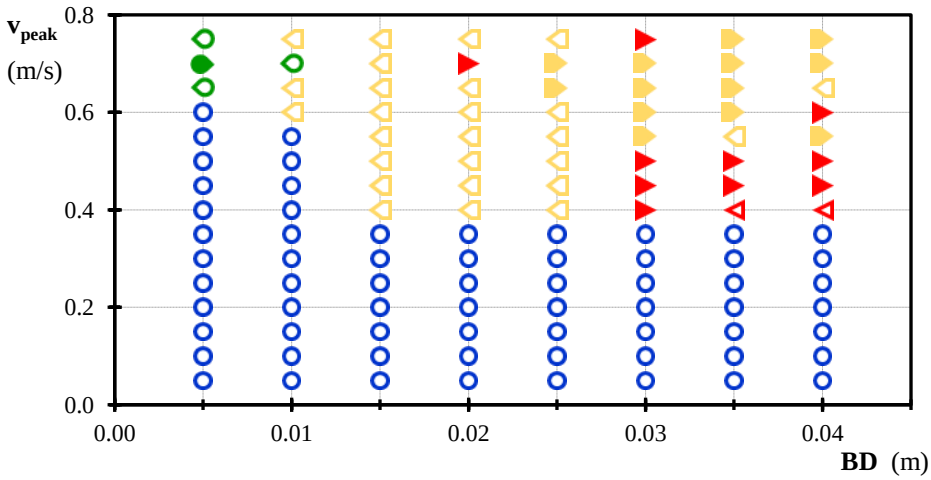

Figure 19. Modes of overturning of a three-block structure (Scale 2) from computational simulation study

Multi Block Study – comments on scaling effect

In a similar way as was shown earlier for a single block, experimental results from both scales of the three block stack are plotted in a single, combined graph in Figure 20. The frequency parameter analytically obtained for the case of a single block with corresponding overall dimensions of the stack of three blocks is used to scale the excitation frequency, while the overall mass of the stack is used to scale the input kinetic energy of the system.

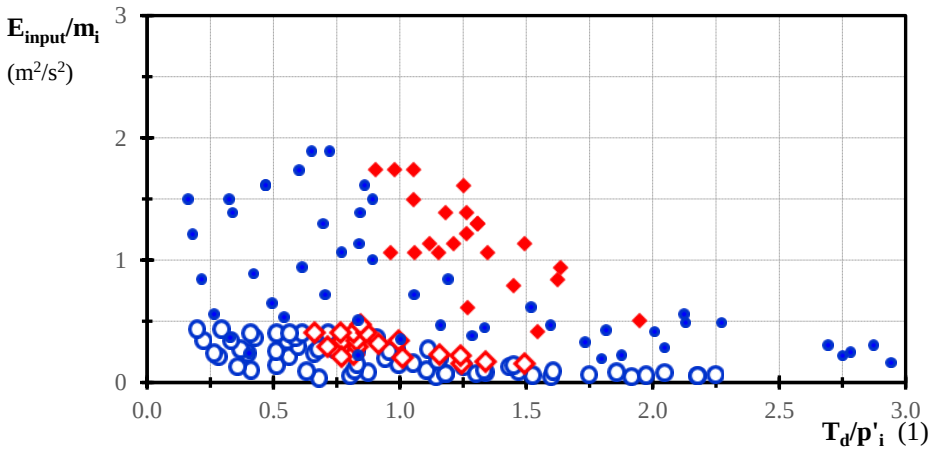

Figure 20. Areas of overturning and no overturning for three-block structure (Scale 1 is represented with filled marks, Scale 2 is represented with empty marks) obtained from experimental study

Computational simulation results from both scales are further shown in Figure 21, with no clear conclusion to be drawn, which implies the need for further study in search of a better scaling parameter for the amplitude of excitation, which would take into account both the mass and geometry attributes (such as size and slenderness), as well as contact conditions.

Author

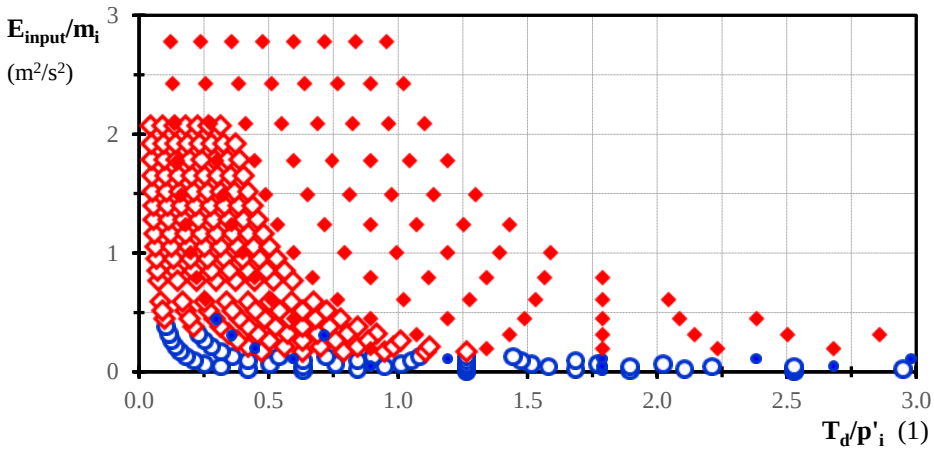

Figure 21. Areas of overturning and no overturning for three-block structure (Scale 1 is represented with filled marks, Scale 2 is represented with empty marks) obtained from numerical study

Excitation signal and detailed study of the overturning modes

During the double impulse experiment, the base excitation history comprises four sections (Figure 22):

a) Initial impact between the projectile and the base (via rubber cushion),

b) Sliding of the base (free travel) with a gradual decrease in the sliding base velocity due to the friction between the sliding aluminium base and the teflon PTFE surface,

c) Second, reverse impact between the sliding base and the stopper (via rubber cushion) and

d) Sliding of the base in the opposite direction, again associated with a decrease in velocity due to the friction between the aluminium base and the teflon PTFE surface.

For all simulations, a constant base acceleration of a finite duration was induced leading to a linear velocity increase, controlled by two parameters - the rise time (which was kept constant at 0.005 sec in all simulations, as the differences were

almost indistinguishable) and the peak base velocity – both parameters experimentally obtained from Aramis results.

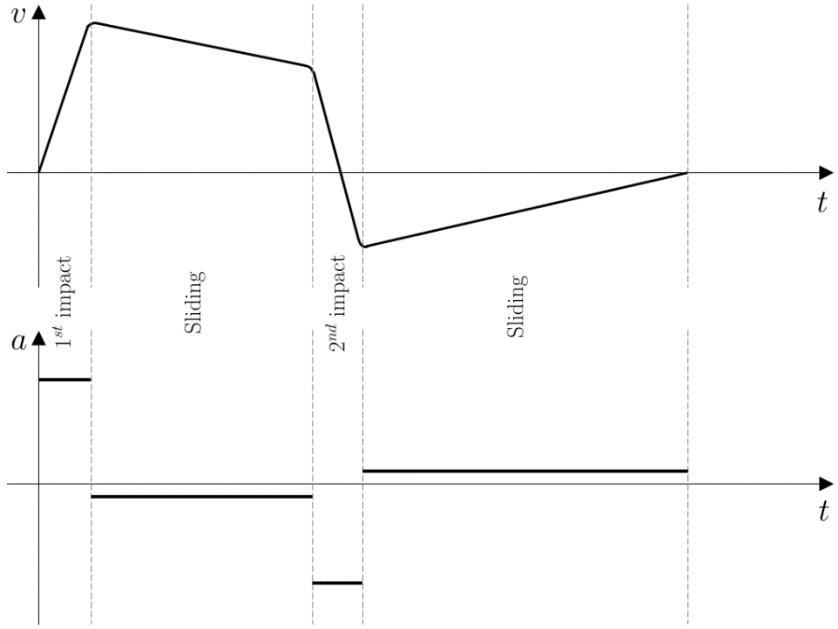

Figure 22. Four sections of the sliding base velocity history, as obtained from the experiments

In earlier paragraphs a simplified characterisation of the final overturning modes was described as the observed outcome of an experiment or a simulation (stable, overturning forward and overturning backward), without considering how these eventual overturning modes have been achieved. Near the transition boundary between the stabilty and instability range in the overtuning graphs, it is to be expected that small changes in the excitation condition (projectile velocity and/or base to stopper distance) may influence the overturning mode.

Single Block Overturning Modes

For a single block, as an illustration, Figure 23 and Figure 24 show substantial differences of the eventual overturning modes for the two cases, which were subject to very similar projectile velocities. It can be noted that these differences in the outcome are primarily associated with the actual timing of the reverse shock

(i.e. at what stage of rocking does the reverse impact with stopper take place) which in turn is obviously related to different distances between the base and the stopper.

The graphs in Figure 23 (detail extracted by zooming Figure 9) show the case where the single block started rocking about its left edge due to the initial acceleration of the base, but when the reverse impact of the base with the stopper happened, the block started rocking back and finally ended rocking around its right corner, eventually overturning to the right side.

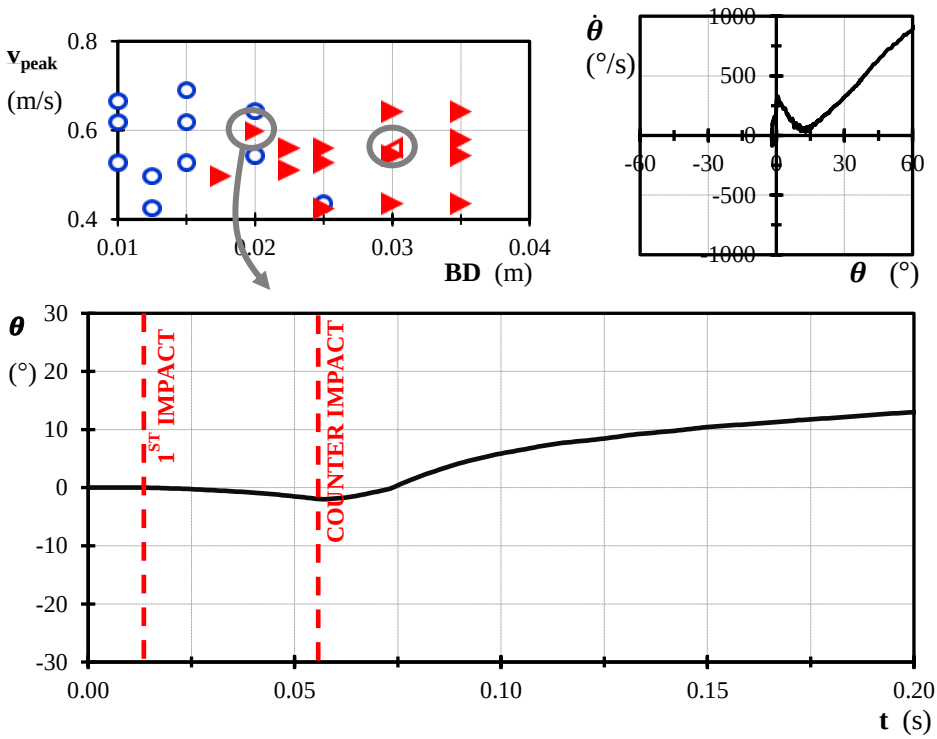

Figure 23. Phase plane view (above on the right) and rotation time history (below) of the experiment of a single block (Scale 1) motion with initial conditions v_{peak}=0.59 m/s, BD=2.0 cm

The graphs in Figure 24 show the case with a very similar base velocity, but a larger distance between the base and the stopper (hence a longer time of free travel of the base), where the block started rocking around its left edge and when the reverse impact happened it started to rotate back to its initial vertical position -

however the angular velocity at that instant was such that the block ended eventually overturning to the left side.

Both experimental cases are accompanied by a phase plane plot, which would enable the detection of any attractor points in such dynamic behavior.

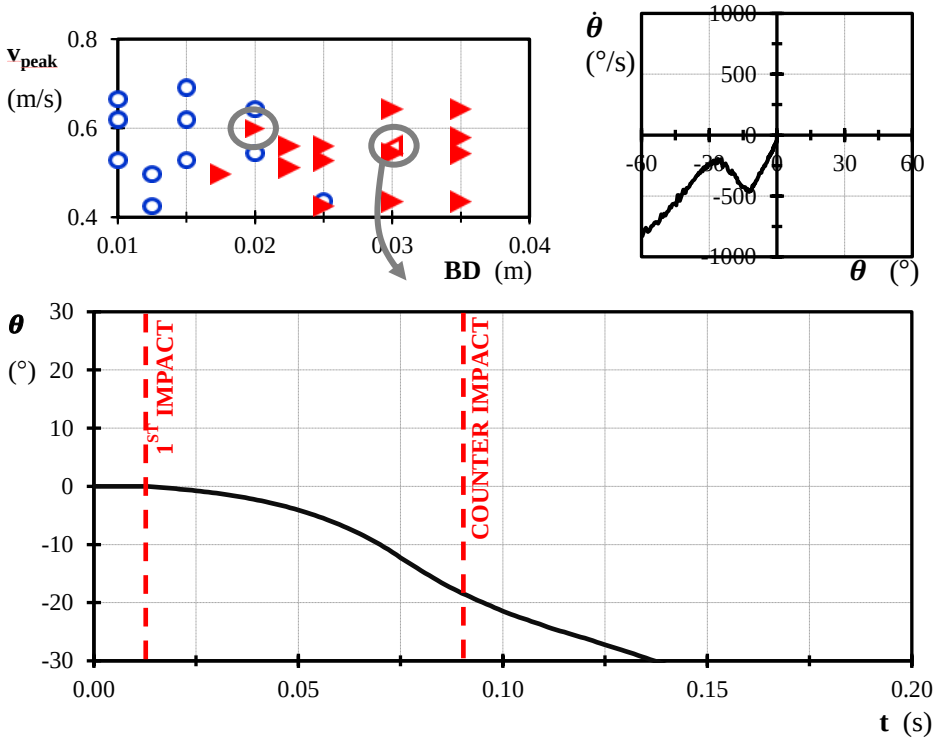

Figure 24. Phase plane view (above on the right) and rotation time history (below) of the experiment of a single block (Scale 1) motion with initial conditions v_{peak}=0.56 m/s, BD=3.0 cm

Tracing the details of the overturning histories provides not only an additional angle in the interpretation of the reasons for the eventual overturning modes (the time instant of the reverse impact while the block is either leaning forward or backward as a result of the initial shock) - it also provides additional detailed information and forms a part of the benchmarking and validation of various simulation frameworks.

Three Block Stack Overturning Modes

Overturning modes of the three block stack also depend significantly on the timing of the reverse impact with the stopper. Figure 25 and Figure 26 illustrate the significant differences between the overturning modes of the stack with the same initial velocity of the base, but with a perturbation in the BD distance.

The experiment shown in Figure 25 shows a case where the entire stack started rotating around the left edge, but the reverse impact happened exactly in time to produce a small push to the left side so that the bottom block started rotating backwards and finally ended up in the vertical position, while the two upper blocks overturned to the left side.

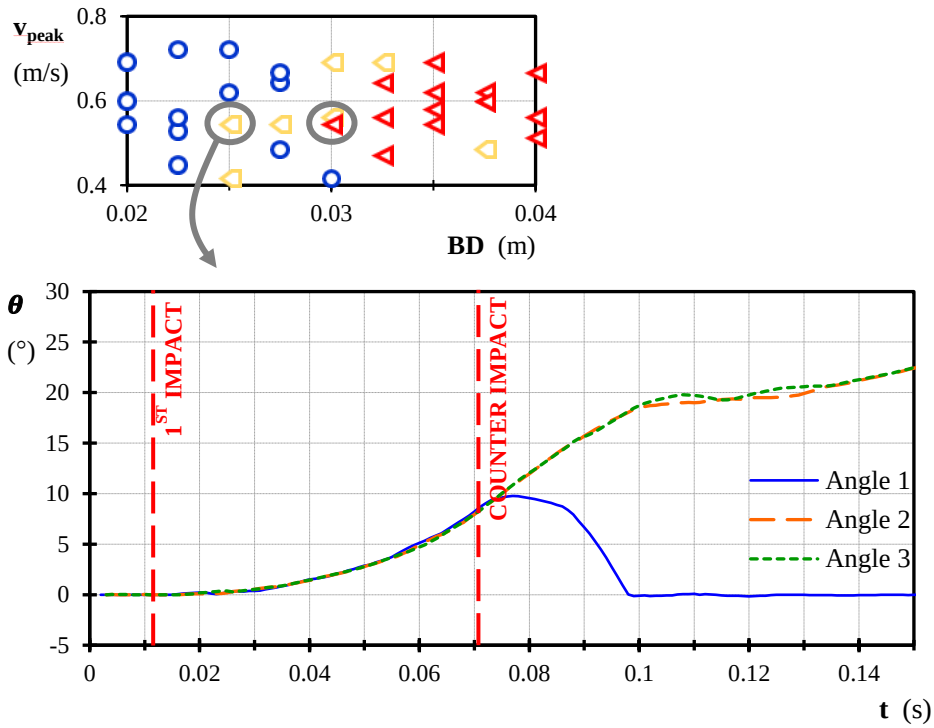

Figure 25.Rotation time history of the experiment of a three block stack (Scale 1) motion with initial conditions v_{peak}=0.54 m/s, BD=2.5 cm

The experiment shown in Figure 26 started with a behaviour similar to the case just described, but the reverse impact happened later (due to the larger BD distance) and even though the bottom block clearly experienced a decrease in

angular velocity (indicating a tendency to rotate in the opposite direction) the entire stack ended up overturning to the left.

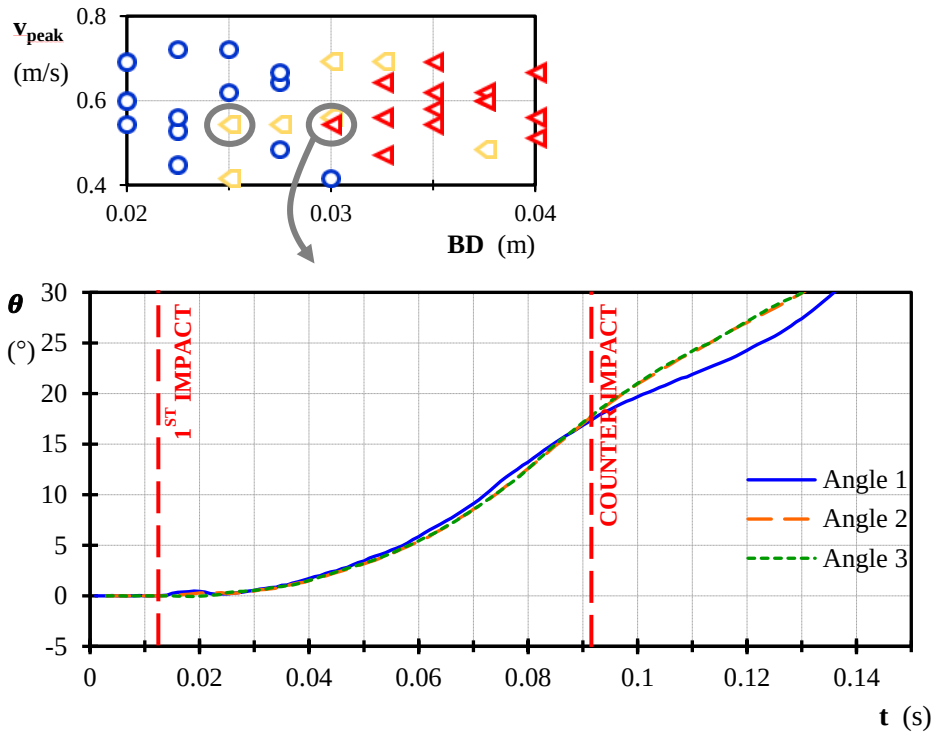

Figure 26. Rotation time history of the experiment of a three block stack (Scale 1) motion with initial conditions v_{peak}=0.54 m/s, BD=3.0 cm

The results for the two cases described above are further illustrated on Figure 27 (corresponding to the case shown earlier in Figure 25) and Figure 28 (corresponding to the case shown earlier in Figure 26) by means of the rotation phase plane views for the entire stack comprising three blocks, as well as for each of the three blocks individually. Rotation phase plane view enables an easier insight into the dynamic behaviour of each of the bodies within a multiple body system during the course of the experiment (or simulation). Rotation phase plane view of the whole stack and of the bottom block in Figure 27 shows clockwise rocking motion of the bottom block (as well as the upper two blocks) up until the time the counter-impact takes place, which is followed by counter-clockwise direction of rotation of the bottom block leading finally to a stable end state of the

bottom block, while the top two blocks overturn, hence this case leads to a partial stack overturning. Corresponding rotation phase plane views in Figure 28, where the BD distance is larger, show the initial clockwise rocking motion of the three blocks up until the counter-impact takes place, which is again followed by a counter-clockwise motion and a tendency to a stable end state. Since the BD distance is larger such a stable position is not reached and a global overturning of the stack as the whole takes place.

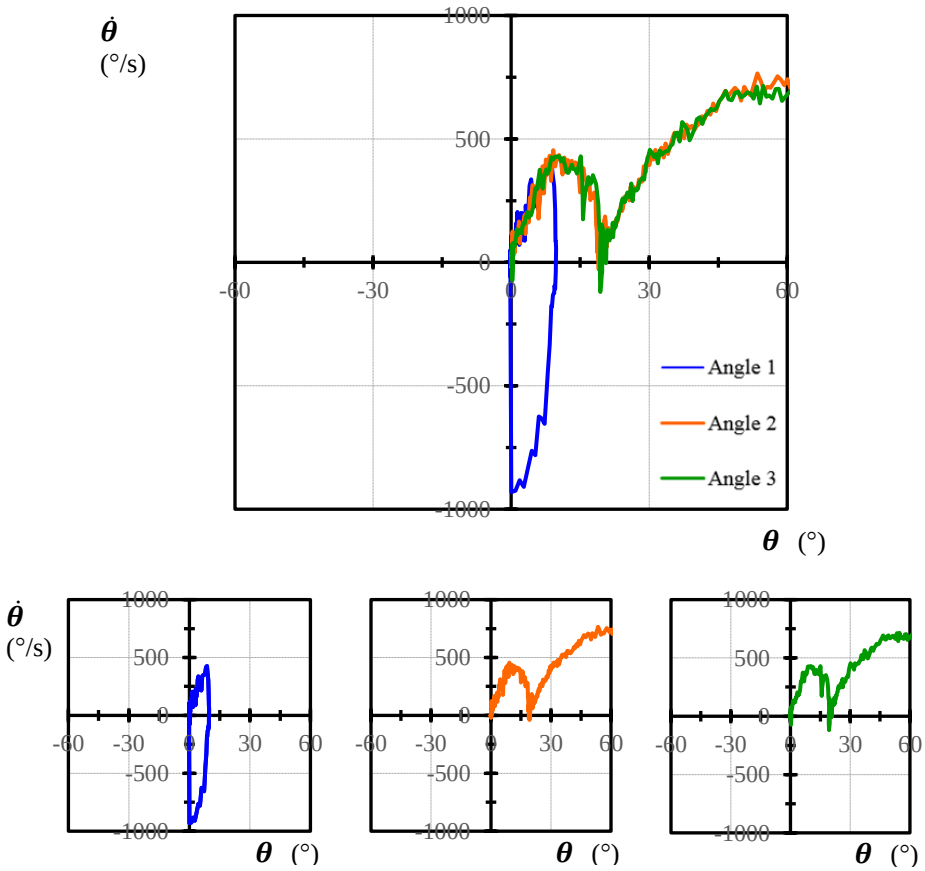

Figure 27. Rotation phase planes of the experiment of a three block stack (Scale 1) motion with initial conditions v_{peak}=0.54 m/s, BD=2.5 cm for the whole stack (top graph) and each of the blocks (bottom three graphs)

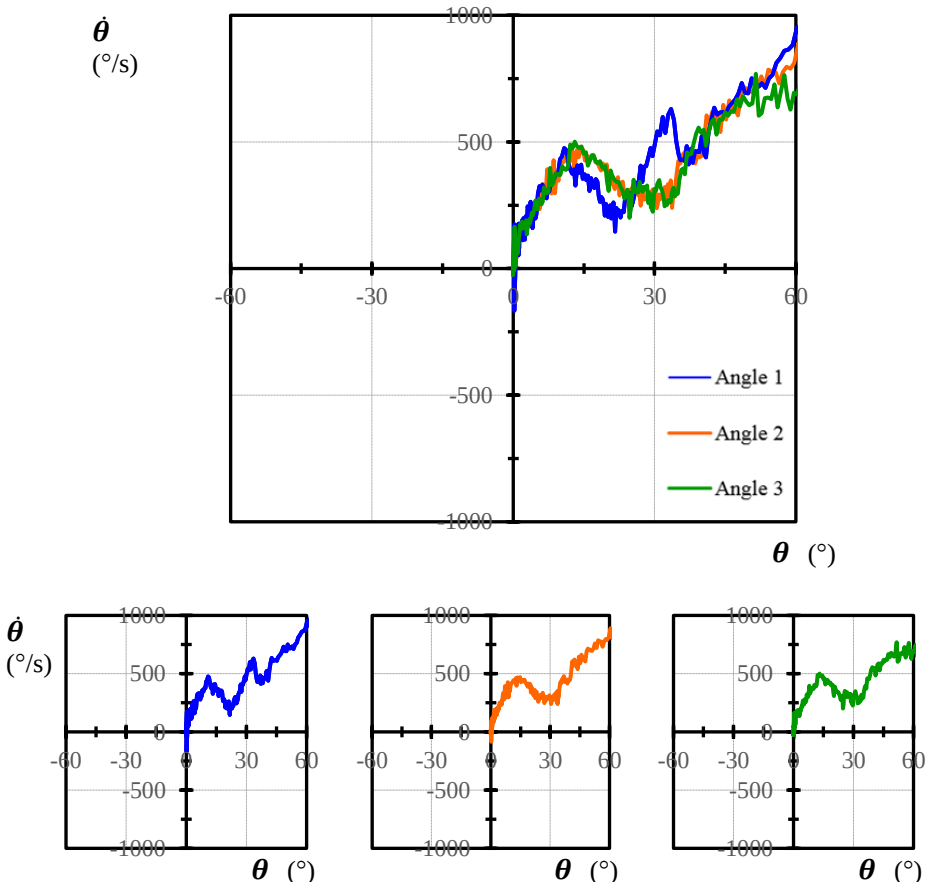

Figure 28. Rotation phase planes of the experiment of a three block stack (Scale 1) motion with initial conditions v_{peak}=0.54 m/s, BD=3.0 cm for the whole stack (top graph) and each block (bottom three graphs)

Conclusions

Preliminary results of both experiments and computational simulations, related to the single block and the multiple block stacks overturning study due to the controlled double pulse excitation are given. A particular attention is given to the excitation conditions (impulse intensities and time delay between the initial and reverse impulse) leading to a partial overtopping mode.

The coarse, predominantly descriptive, characterisation of the eventual overturning modes was augmented by a more detailed study tracing the manner the eventual overturning modes have been achieved. Although broad agreement between the experiments and simulations is achieved and the simulations indicate similar qualitative behaviour as observed in the experiments, further studies are clearly needed. It is believed that the noted differences between the simulation and experimental results stem from the manner the energy dissipation mechanisms on the inter block interfaces as well as on the block-base interface are accounted for, as during the NSCD simulations of rocking behaviour they are dealt with through point wise restitution coefficients. Additional sources emanate from the difficulties and imperfections to manually align the blocks along the same plane, as well as on top of one another during experiments, and the inability to completely prevent sliding motion between the bodies by means of rough surfaces.

The results of the scaling study to render the observed overturning modes dimensionless are inconclusive and require further research, starting with obtaining a series of experimental (and computational) results of dynamic behaviour of a single block and three block stack on a third (larger) scale due to double impulse type base excitation.

Acknowledgements

This work is done as a part of scientific project 3/13 „Evidence based characterisation of dynamic sensitivity for multiblock structures – computational simulation and experimental validation“ (mbsDynamic) supported by Unity Through Knowledge Foundation and in collaboration with University of Oxford and University of Durham, and scientific project HRZZ-1631 "Configuration-dependent approximation in non-linear finite-element analysis of structures“ (CANFAS) supported by Croatian Science Foundation.

Bibliography

Cundall, P.A. and Strack, O.D.L. (1979). *A distinct element model for granular assemblies*. Geotechnique, 29: 47–65.

Dimitrakopoulos, E.G. and DeJong, M.J. (2012) *Revisiting the rocking block: closed-form solutions and similarity laws*. Proc R Soc A Math Phys Eng Sci 468(2144): 2294–318.

Hogan, S. (1994). *Slender Rigid Block Motion*. J. Eng. Mech. 10.1061/(ASCE)0733-9399(1994)120:1(11), 11-24.

Housner, G.W. (1963). *The behavior of inverted pendulum structures during earthquakes*. Bull Seismol Soc Am: 53(2):403–17.

Jean, M. (1999). *The non-smooth contact dynamics method*. Computer Methods in Applied Mechanics and Engineering, vol. 177, no. 3-4: pp. 235–257.

Kounadis, A.N., Papadopoulos, G.J., Cotsovos, D.M. (2012). *Overturning instability of a two-rigid block system*. Z. Angew. Math. Mech.

Koziara, T. and Bićanić, N. (2011) *A distributed memory parallel multibody Contact Dynamics code*. Int J Numer Methods Eng. 87(March): 437–56.

Lopez Garcia, D. and Soong, T.T. (2003). *Sliding fragility of block-type non-structural components. Part 1: Unrestrained components*. Earthquake Engng Struct. Dyn. 32: 111–129.

LS-DYNA - https://en.wikipedia.org/wiki/LS-DYNA

Makris, N.R. (1998). *Rocking response and overturning of equipment under horizontal pulse-type motions*. Berkley. Report PEER-1998/05 Pacific Earthqiake Research Center, University of California.

MbH G. Aramis - User Manual - Software. 49(0).

Peña, F., Campos-Costa, A. (1992). *Experimental dynamic behavior of free standing multi- block structures under seismic loadings*. Metrology Systems: 1-39.

Pena, F., Prieto, F., Laurenço, P.B., Campos-Costa, A. (2006). *Dynamical behaviour of rigid block structures subjected to earthquake motion*. New Delhi. Structural Analysis of Historical Constructions: 707–14.

Pickerd, V. (2013). *Optimisation and Validation of the ARAMIS Digital Image Correlation System for use in Large-scale High-strain-rate Events*.

Psycharis, I.N. (1990). *Dynamic behaviour of rocking two-block assemblies. Earthquake Engineering and Structural Dynamics*.

Psycharis, I.N. and Jennings, P.C. (1983). *Rocking of slender rigid bodies allowed to uplift*. Earthquake Engineering and Structural Dynamics, Vol. 1: 57-76.

Qamaruddin, M., Chandra, B., Arya, A.S. (1984). *Dynamic testing of brick building models*. (ii):353–65.

Radjai, F. and Richefeu, V. (2009). *Contact dynamics as a nonsmooth discrete element method*. Mech Mater 41(6): 715–28.

SOLFEC - Computational contact dynamics - Google Project Hosting https://code.google.com/archive/p/solfec/ [cited 2015 Nov 2].

Spanos, P.D., Roussis, P.C., Politis, N.P.A. (2001). *Dynamic analysis of stacked rigid blocks*. Soil Dynamics and Earthquake Engineering 21: 559-578.

UDEC&3DEC, ITASCA - http://www.itascacg.com/software/udec

Yim, C-S., Chopra, A.K., Penzien, J. (1980) *Rocking response of rigid blocks to earthquake.* Earthquake engineering and structural dynamics, vol.8: 565-587.

Zhang, J. and Makris, N. (2001). *Rocking response of free-standing blocks under cycloidal pulses*. Journal of engineering mechanics: 473-483.